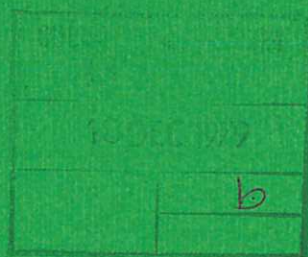




UKAEA

Preprint

A BORON NITRIDE CONTINUOUS WAVE
CARBON DIOXIDE WAVEGUIDE LASER FOR
OPTICALLY PUMPING HEAVY WATER



D. E. EVANS

S. L. PRUNTY

M. C. SEXTON

CULHAM LABORATORY
Abingdon Oxfordshire

1979

This document is intended for publication in a journal or at a conference and is made available on the understanding that extracts or references will not be published prior to publication of the original, without the consent of the authors.

Enquiries about copyright and reproduction should be addressed to the Librarian, UKAEA, Culham Laboratory, Abingdon, Oxfordshire, England

A BORON NITRIDE CONTINUOUS WAVE CARBON DIOXIDE WAVEGUIDE LASER FOR OPTICALLY PUMPING HEAVY WATER

D E Evans, S L Prunty* and M C Sexton*

UKAEA, Culham Laboratory, Abingdon, Oxon, OX14 3DB, UK
(Euratom/UKAEA Fusion Association)

A B S T R A C T

Boron Nitride has been used to fabricate a 1 cm^3 CW CO_2 capillary waveguide laser which operates at 130 torr gas pressure, and generates 7 W of 10 micron radiation untuned and up to 3 W on individual grating-selected emission lines. Pressure broadened gain profiles are limited to ± 200 MHz from line centre by longitudinal cavity mode spacing. Increased absorption of the 9 micron band R(22), R(12) and P(32) lines by D_2O vapour is observed as these lines are tuned across the broadened gain profile towards their respective D_2O absorptions.

* University College, Cork, Ireland

INTRODUCTION

The large output power and narrow bandwidth obtainable from pulsed CO_2 TEA laser-pumped heavy water (D_2O) at $385\text{ }\mu\text{m}$, $114\text{ }\mu\text{m}$, and $66\text{ }\mu\text{m}$, makes the latter a strong candidate for collective scattering measurements in fusion research plasma experiments⁽¹⁾. Continuous generation of radiation at these wavelengths for use as local oscillator power in a heterodyne receiver presents a difficulty, however, owing to mismatches between the C W CO_2 laser emission lines and the D_2O absorptions amounting to 318 MHz, 680 MHz, and 1500 MHz respectively⁽²⁾, and as a result, such a C W D_2O laser has not as yet been reported*.

The tuning range in conventional C W CO_2 lasers is about 60 MHz full width, too little to overcome these mismatches. However, if a CO_2 laser is constructed in the form of a capillary (= 1 mm bore) dielectric waveguide⁽³⁾, advantage can be taken of the ability of a narrow bore tube to increase discharge cooling and reduce bottle-necking in the lower laser level. Operating the discharge at much increased pressure results in increasing collision-broadened bandwidth, gain, and output power per unit volume. The enhanced bandwidth allows one to tune the cavity resonance several hundred MHz across the laser transition, itself selected by a diffraction grating, by changing the cavity length. The tuning range is given by⁽⁴⁾

$$2|\nu - \nu_0| = \Delta\nu \left[\frac{g_0 L}{\ln \frac{1}{\sqrt{r_1 r_2}}} - 1 \right]^{\frac{1}{2}} \quad \dots(1)$$

where g_0 is the small signal gain at line centre,

L is the discharge length,

* Recently Danielewicz and Weiss (Opt Commun 27 98 1978) obtained C W laser emission from D_2O at $112.6\text{ }\mu\text{m}$ and $94.5\text{ }\mu\text{m}$ using a sequence band CO_2 laser. However these are not among the lines which give high laser output under pulse pumping.

r_1 and r_2 are the reflectivities of the laser cavity end mirrors, and the width of the collision-broadened Lorentz line is given by⁽⁴⁾

$$\Delta\nu \text{ (MHz)} = 7.58 \left(f_{\text{CO}_2} + 0.73 f_{\text{N}_2} + 0.6 f_{\text{He}} \right) p(\text{torr}) \sqrt{\frac{300}{T(^{\circ}\text{K})}} \quad \dots(2)$$

where f_x is the fraction by volume of gas x

p is the pressure, and

T is the discharge temperature.

It can be seen that decreasing the discharge temperature increases the tuning range both by increasing the line centre gain g_0 through reduction of the population of the lower laser level, and by increasing the collision frequency. The greatest possible rate of transfer of heat from the discharge is accordingly required to maximize tuning range and output power, hence high thermal conductivity ceramic is indicated for the discharge tube. The material chosen must also satisfy the requirement of low propagation loss in a hollow waveguide having transverse dimensions large compared to the wavelength⁽⁵⁾. Beryllium oxide appears to be the best material in both respects, but difficulties are encountered in the fabrication of lasers from BeO owing to the high toxicity of its airborne particles released during machining. For this reason, we have elected to construct our waveguide lasers from boron nitride (BN) which can be machined with safety, and whose suitability for waveguide laser construction has already been demonstrated⁽⁶⁾.

CONSTRUCTION OF THE CO₂ WAVEGUIDE LASERS

Two lasers have been constructed with the guide in each case consisting of a square channel (1.7 mm x 1.7 mm) having discharge lengths 12 cm and 24 cm respectively. A straight guide is first machined in a 1" x 1" block of BN using conventional milling techniques, thereafter the guide is formed by inserting an additional slab of BN, and the assembly is

epoxied together to form a vacuum tight seal (Figure 1). Machinable glass ceramic holds the electrodes in position and is also used for the end flanges and the gas feedthroughs. To minimize the overall voltage necessary to produce a discharge, as well as to avoid mirror or window damage from positive ion bombardment, a four electrode geometry is employed. Electrodes consist of tungsten pins brought through holes in the sides of the guide, with the centre electrodes connected via ballast resistors to negative HV and with the end electrodes near ground potential. Simultaneous striking of both discharge legs has been achieved by connecting small resistors between the end electrodes and ground. The optimum discharge current in each leg was the order of 4 mA. A continuously flowing gas mixture (approximately $\text{He:N}_2:\text{CO}_2$ 8:1:1, more He being added at higher pressures) is introduced at the centre of the guide and evacuation takes place through holes near the end flanges. Each laser is cooled by conduction through a water-cooled aluminium block, with which it is in close contact.

A schematic of the smaller laser is shown in Figure 1, while Figure 2 is a photograph of one end of the guide channel.

PERFORMANCE

LONG WAVEGUIDE LASER

The laser cavity was first formed by flat mirrors placed 12 mm from the waveguide ends, one being gold coated for 100% reflectivity, the other being an uncoated germanium flat through which the laser radiation emerged. Laser power versus pressure and discharge current measured in this configuration is shown in Figure 3. It can be seen that the optimum pressure for maximum output power occurs in the 120-130 torr region, in agreement with previously reported measurements for a similar system⁽⁷⁾. The highest power obtained was 7.6 W with discharge parameters 10 kV and 4.6 mA in each discharge leg. This was equivalent to 0.32 W cm^{-1} , and an electrical-to-optical efficiency of 8.3 %.

The angular distribution of radiation from the end of the guide was measured by traversing a vertical slit across the beam in the far field, and performing an Abel inversion on the resulting data. The near-Gaussian distribution which emerged, shown in Figure 4, is consistent with predominantly single-mode operation.

By replacing the gold-coated mirror with a 150 line/mm grating, power up to 3 W was obtained on individual emission lines in the 9 μm and the 10 μm bands,

Frequency tuning within one line was accomplished by means of a 92% reflecting ZnSe mirror mounted on a commercial piezo-electric translator (PZT). The tuning range obtained was measured by estimating the fraction of the optical cavity free spectral range (454.5 MHz for the 33 cm cavity) over which laser oscillation was maintained on a single line. Occasionally laser emission was observed to jump to lines adjacent to the selected one during PZT tuning, but only one line oscillated at a time. Improved emission line discrimination is anticipated when the beam from the guide end is expanded before it reaches the grating, increasing the effective resolution of the latter. With the arrangement described, a tuning range of the order of 400 MHz has been obtained.

The optical cavity itself imposes a tuning range limitation owing to competition for available gain between neighbouring cavity resonances. As a result, a new longitudinal mode appears as soon as the cavity frequency tuning reaches one-half the longitudinal mode spacing. The maximum frequency offset from line centre is therefore

$$|\nu - \nu_0|_{\text{max}} = \frac{c}{4d} \quad \dots(3)$$

where c is the velocity of light and d is the mirror separation. That the tuning range actually measured was rather less than that expected from equation (3), i.e. 400 MHz instead of the expected 454 MHz, may be due to losses in the guide reducing the effective reflectivity, $\sqrt{r_1 r_2}$ in equation (1).

As an example of the laser's capabilities, we have demonstrated absorption in heavy water vapour on the R(22), the R(12), and the P(32) lines over a 400 MHz frequency range as a function of D₂O pressure. The measurements were performed by passing the CO₂ laser beam through a 50 cm long cell containing the D₂O vapour. Transmitted power was plotted as a function of ramp voltage applied to the PZT on an XY recorder for different pressures. Figure 5 illustrates the result in the case of the R(22) line. The asymmetric shape of the absorption curves is attributed to wing absorption occurring more strongly on the left hand side of the emission peaks. Assuming a Lorentzian absorption profile⁽⁸⁾ the calculation detailed in the Appendix determines that the absorption line centre lies 310 ± 22 MHz above the R(22) transition in CO₂, and the CO₂ line centre absorption coefficient is $3.8 \times 10^{-3} \text{ cm}^{-1} \text{ torr}^{-2}$. These compare not unfavourably with the previous measured values⁽²⁾ of 318 MHz and $1.8 \times 10^{-3} \text{ cm}^{-1} \text{ torr}^{-2}$. Longer absorption tubes or a higher range of D₂O pressures are required to obtain similar results for the R(12) and P(32) lines.

SHORT WAVEGUIDE LASER

With a 92% reflecting ZnSe coated output mirror and a 100% reflector placed directly on the ends of the waveguide, a maximum output of 1.6 W, representing 10.5% electrical-to-optical conversion efficiency was obtained from this system. The discharge parameters were 1.9 kV and 4 mA in each leg, and the gas pressure in the capillary was 70 torr. To measure the tuning range, the 100% mirror was replaced by a 150 line/mm grating, and a 97% reflectivity output mirror was mounted on the PZT. A tuning range of 550 MHz was obtained at 80 torr with an output power on a single line of about 100 mW. Output power decreased significantly when pressure was increased to try to extend the tuning range.

Tuning range and output power of both laser systems would be increased if more efficient cooling were applied. Burkhardt et al⁽⁹⁾ have measured 70% improvement in output by cooling to -60°C .

If this were done, we estimate from equation (1) that a tuning range in excess of 1 GHz, limited by the mode spacing of the cavity, would result, and this would permit us to achieve line centre absorption in D_2O .

The conflicting requirements of a long discharge to achieve high output power, and a short optical cavity to secure wide tuning range can be reconciled if an intra-cavity etalon is introduced to suppress unwanted longitudinal modes. Calculation suggests that the use of a CdTe etalon in the longer of the two lasers reported here should yield a tuning range of greater than 2 GHz.

CONCLUSIONS

Boron nitride, which combines good heat conduction and electrical insulation properties with ease and safety in machining, has been used in preference to beryllium oxide to fabricate capillary waveguide CO_2 lasers. Such a laser having waveguide dimensions $1.7\text{mm} \times 1.7\text{mm} \times 300\text{ mm}$ operated at 130 torr pressure and 90 W electrical, has generated more than 7 W of $10\text{ }\mu\text{m}$ radiation untuned and in excess of 3 W on individual emission lines selected by intra-cavity grating. The pressure-broadened tuning range of the output was limited by longitudinal cavity mode spacing and cavity losses to about $\pm 200\text{ MHz}$ from line centre. This was improved to $\pm 275\text{ MHz}$ in a 150 mm long laser, but the power radiated was smaller by more than an order of magnitude.

Increased absorption of the emission line R(22) by heavy water vapour as this line was tuned across its pressure-broadened gain profile towards the D_2O absorption has been observed. Absorption in D_2O has also been observed on R(12) and P(32).

ACKNOWLEDGEMENT

The authors wish to thank Mr H H H Watson and Mr D H Wilson of the Applied Physics and Technology Division, Culham, for technical advice and for constructing the waveguides. One of us, S L P, acknowledges an Irish Department of Education Postdoctoral Fellowship. This work is supported by the USAF Office of Scientific Research under Grant AFOSR-76-3077, and the National Board for Science and Technology, Dublin.

REFERENCES

1. T K Plant L A Newman E J Danielewicz T A DeTemple and P D Coleman
Microwave Theory and Tech MTT-22 988 (1974)
D E Evans L E Sharp W A Peebles and G Taylor
Optics Commun 18 479 (1976)
P Woskoboinikow H C Praddaude W J Mulligan D R Cohn and B Lax
J Appl Physics 50 1125 (1979)
2. S J Petuchowski A T Rosenberger and T A DeTemple
IEEE J of Quantum Electronics QE-13 476 (1977)
3. J J Degnan Appl Phys 11 1 (1976)
4. J J Degnan J Appl Phys 45 257 (1974)
5. D R Hall, E K Gorton and M R Jenkins
J Appl Phys 48 1212 (1977)
6. A Papayoanou IEEE J Quantum Electronics QE-13 27 (1977)
7. A Papayoanou ECOM Tech Rep 4430 Sept 1976
and private communication
8. A Yariv "Quantum Electronics" John Wiley and Sons Inc (1976)
9. E G Burkhardt T J Bridges and P W Smith
Opt Commun 6 193 (1972)

APPENDIX

This appendix describes the calculations of the frequency mismatch between CO₂ emission lines and D₂O absorptions, from asymmetry in absorption measured across CO₂ laser pressure-broadened emission profiles.

The fraction $\frac{I}{I_0}$ of CO₂ laser radiation transmitted through a depth S of D₂O vapour is given by:

$$I = I_0 e^{-\alpha S} \quad \dots (A1)$$

where the absorption coefficient α is assumed to be dominated by pressure-broadening, and so is Lorentzian^[8]:

$$\alpha(\nu) = \left(N_1 \frac{g_2}{g_1} - N_2 \right) \frac{\lambda^2 A_{21}}{8\pi^2} \frac{\left(\frac{\Delta\nu_a}{2} \right)}{(\nu - \nu_a)^2 + \left(\frac{\Delta\nu_a}{2} \right)^2} \quad \dots (A2)$$

Here ν_a is the frequency at the centre of the D₂O absorption line and $\Delta\nu_a$ is its width at half-height. The other quantities have their usual spectroscopic meanings. As both the population-of-states term and $\Delta\nu_a$ are proportional to pressure p, the foregoing can be written:

$$\alpha(\nu) = \frac{\Gamma^2 \alpha(\nu_a) p^2}{4(\nu - \nu_a)^2 + \Gamma^2 p^2} \quad \dots (A3)$$

where Γ is the constant of proportionality between $\Delta\nu_a$ and p.

At low pressure and far from absorption line centre $4(\nu - \nu_a)^2 \gg \Gamma^2 p^2$. With this provision, combining (A1) and (A3) and writing:

$$\nu - \nu_a = (\nu - \nu_e) + (\nu_e - \nu_a)$$

where ν_e is the centre of the CO₂ emission line,

$$(\nu - \nu_e) = -(\nu_e - \nu_a) + \frac{\Gamma p}{2} \sqrt{\alpha(\nu_a) S} \left(\ln \frac{I_0}{I} \right)^{-\frac{1}{2}} \quad \dots (A4)$$

This has the form of a straight line $y = a_0 + a_1 x$ with $y = \nu - \nu_e$ and $x = (\ln I_0/I)^{-\frac{1}{2}}$. The result for R(22) with p = 1 torr is plotted in Figure 6. The y-intercept $a_0 = -(\nu_e - \nu_a)$ is found to be 310 ± 22 MHz in this case.

The slope of the straight line gives a value for $\Gamma^2 \alpha(\nu_a)$, in this example, $(1.4 \pm 0.3) \times 10^3 \text{ MHz}^2 \text{ torr}^{-2} \text{ cm}^{-1}$. Hence absorption at the centre of the CO₂ line is $(3.7 \pm 0.9) \times 10^{-3} \text{ torr}^{-2} \text{ cm}^{-1}$.

Combining (A1) and (A3) with no restriction on p or v leads to:

$$\left(\ln \frac{I_o}{I} \right)^{-1} = \frac{\left[(v - v_e) + (v_e - v_a) \right]^2}{\left(\frac{\Gamma_p}{2} \right)^2 \alpha(v_a) S} + \frac{1}{\alpha(v_a) S} \quad \dots (A5)$$

and the y-intercept in this case gives a value for $\alpha(v_a)$, the absorption coefficient at the centre of the D_2O absorption. In our work, the error on a_o was too large to allow a meaningful value of $\alpha(v_a)$ and so of Γ to be calculated.

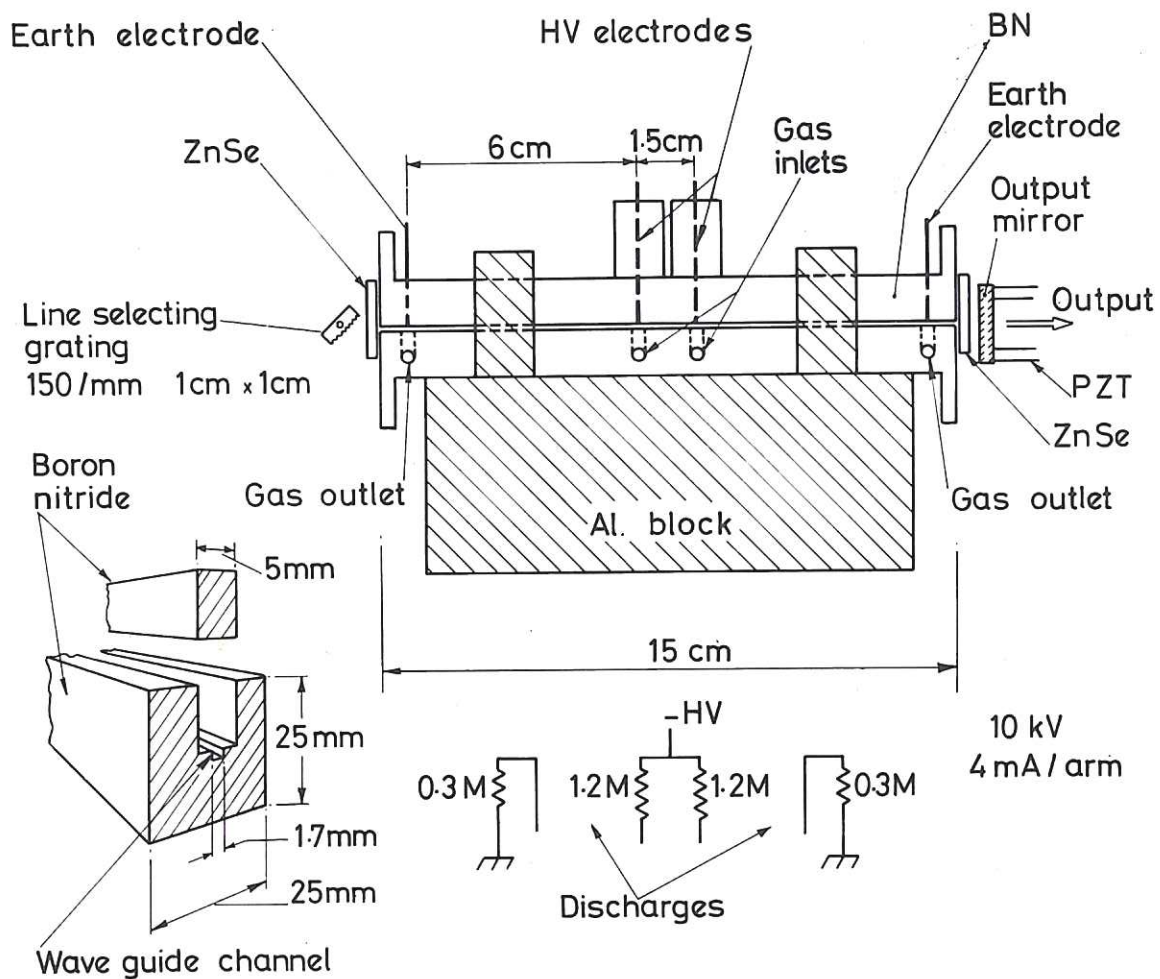


Fig.1 Side elevation of the 12cm discharge waveguide laser. Also shown, method of construction of the waveguide channel, to the left, and electrical discharge circuit.

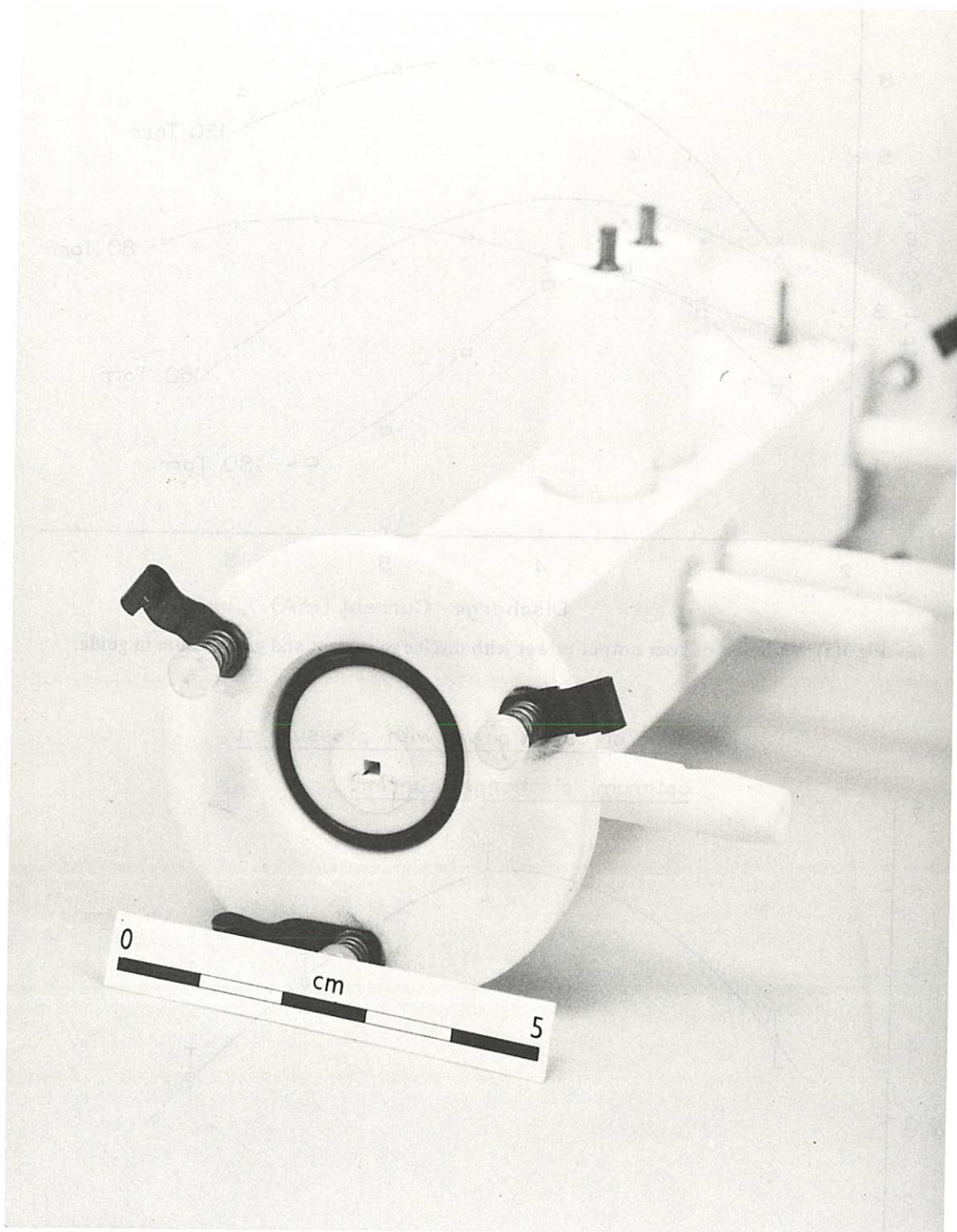


Fig.2 Photograph of the end of the BN waveguide, showing one end of the guide channel.

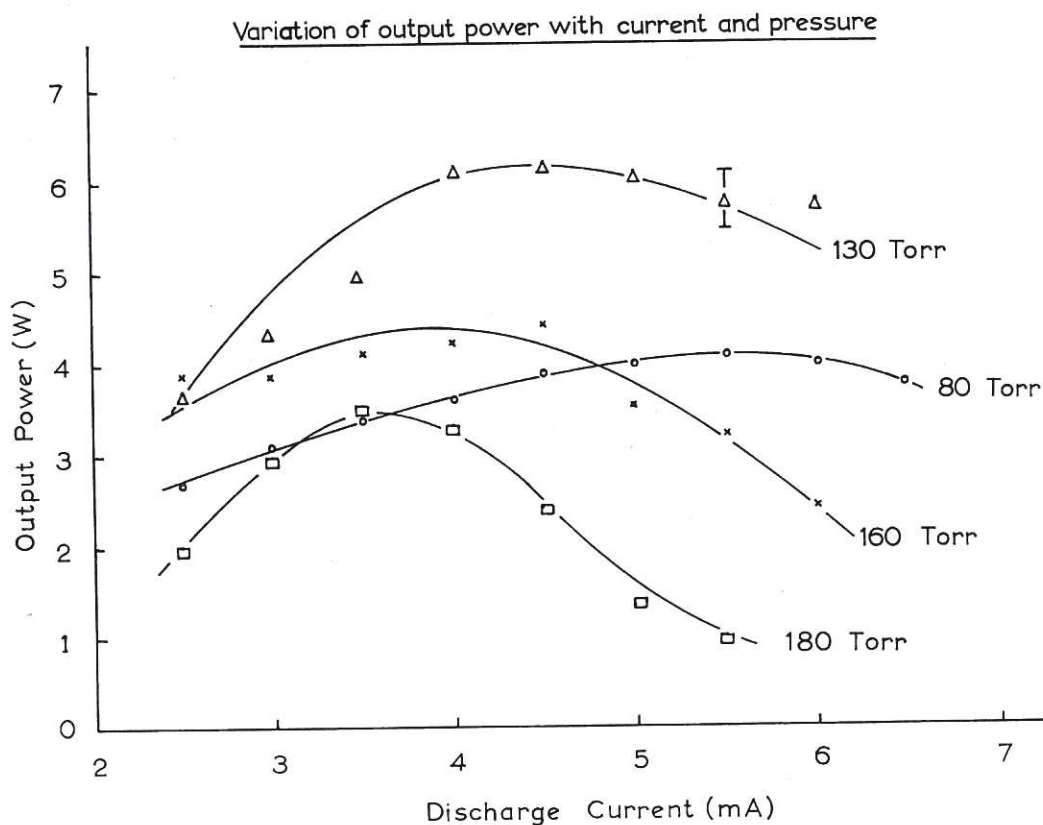


Fig.3(a) Variation of laser output power with discharge current and gas pressure in guide.

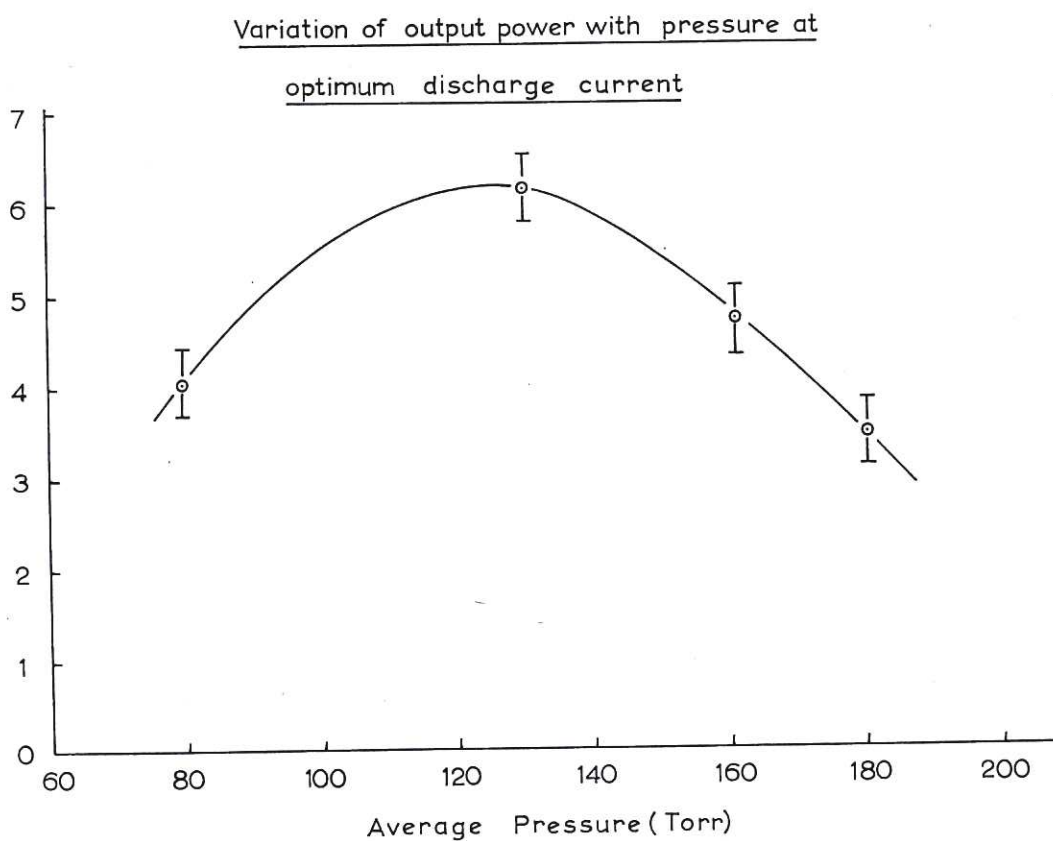


Fig.3(b) Variation of laser output power with pressure at optimum discharge current (which is different for each value of pressure).

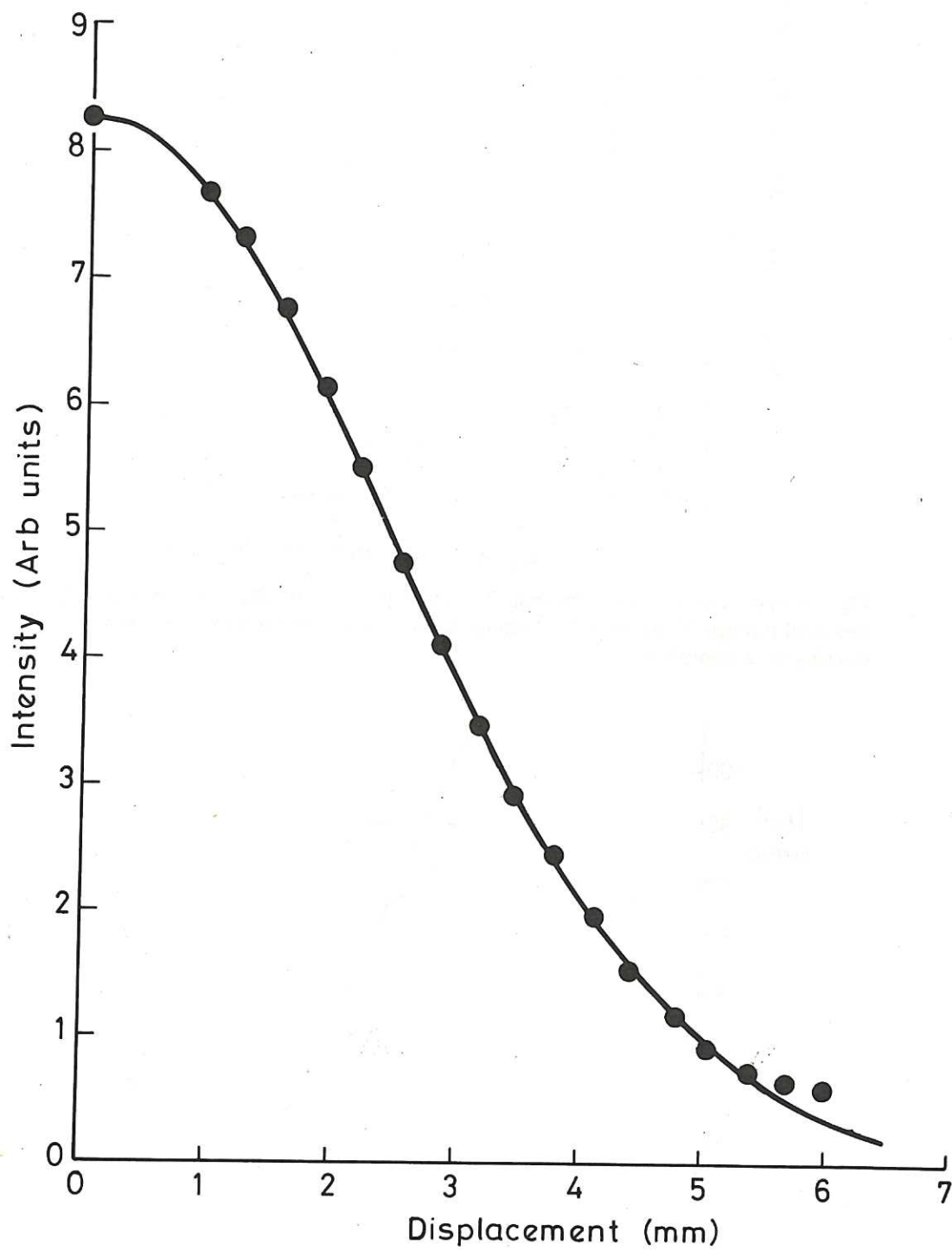


Fig.4 Far field radiation pattern. The continuous curve is the best fit Gaussian.

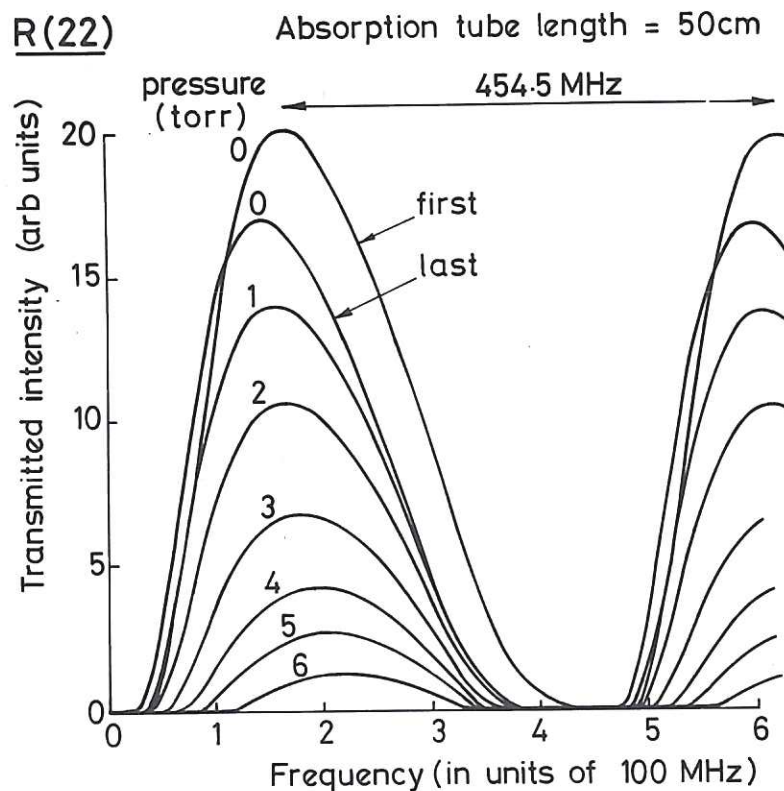


Fig.5 Output of laser on the $9\mu\text{m}$ band R(22) line, piezo-electrically tuned in frequency, measured through 50cm cell of D_2O vapour at the pressure indicated on each curve, showing wing absorption.

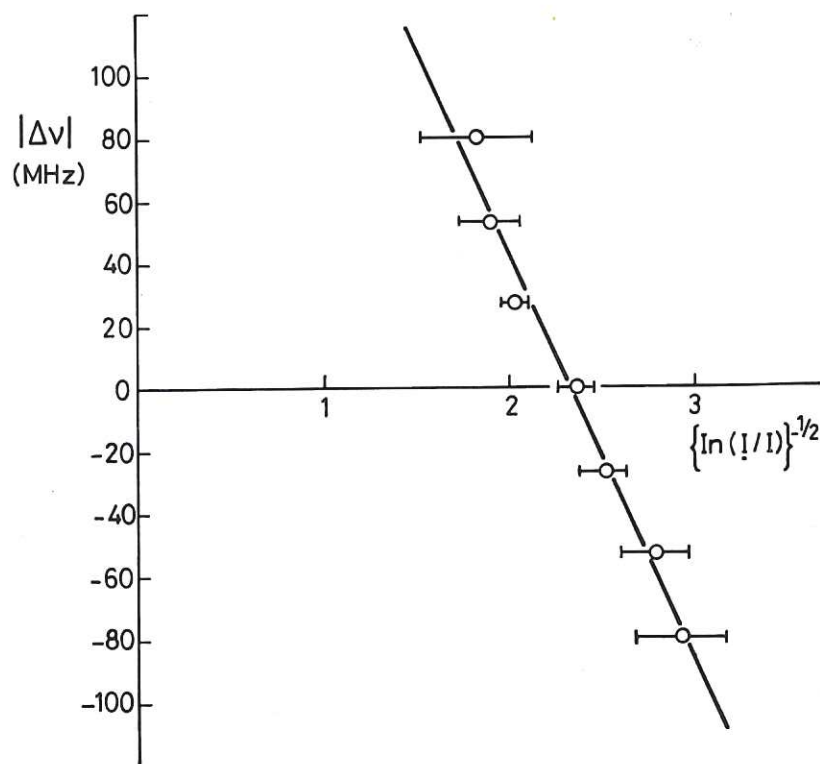


Fig.6 Frequency mismatch between $9\mu\text{m}$ band R(22) emission from CO_2 and corresponding absorption in D_2O . Graph shows $(\nu - \nu_e)$ plotted against $(\ln \frac{I_0}{I})^{-1/2}$.

The y-intercept defines the emission-absorption mismatch to be $310 \pm 22\text{MHz}$. D_2O pressure = 1 torr.

